Morphology and possible volcanic origin of sub-kilometer domes in the Arrhenius Region, Mars

Reina L. Foxx
Department of Geological Sciences, California State University Fullerton, Fullerton, CA 93740
Faculty Sponsor: John D. Cooper, California State University, Fullerton

Carrie R. Brugger
Department of Geology, The Colorado College, Colorado Springs, CO 80946
Faculty Sponsor: Jeffrey Noblett, The Colorado College, Colorado Springs

OVERVIEW

Mapping part of an extensive field of sub-kilometer domes in the Arrhenius Region of Mars has revealed characteristics similar to some terrestrial volcanic fields. Important for this recognition is the identification of a veneer of sediments whose erosion by aeolian deflation has exposed the domes. There is compelling evidence to support a fracture control for emplacement of the domes because elongate dome long-diameter orientations are nearly identical to those of fractures and a trough in the region. In a volcanic context the two most plausible models for this dome field are cinder cones and table mountains; the choice is dependent upon identifying the time of dome emplacement relative to deposition of the sediments.

INTRODUCTION

The 36,000 km^2 Arrhenius Region is located in the southern hemisphere of Mars east of Hellas Planitia between 235° and 240° east longitude and 40° to 45° south latitude. Several terrestrial analogs previously have been proposed to explain the origin of the sub-kilometer domes in this region. These include: diatremes (Hodges, 1994), cinder cones (Hodges, 1979; Plescia 1980; Wood, 1979), table mountains (Hodges, 1979), pingos (Judson and Rossenbacher, 1979) and pseudocraters (Hodges, 1979; Allen, 1979; Frey, et al, 1979; Frey and Jarosewich, 1981). The domes likely formed during the Amazonian Era (Hodges and Moore, 1994), which began approximately 1.8 billion years ago. Since then, a variety of processes may have dramatically altered the appearance of this region. For example, extensive aeolian erosion and deposition occurred during the Noachian and Early Hesperian periods in the southern hemisphere (Tanaka and Leonard, 1995).

In this study, we rigorously test the volcanic origin hypothesis by comparing statistical and morphological data from domes in the Arrhenius Region with several terrestrial volcanic dome fields (Tibaldi, 1995). The data utilized in this study were obtained from digital images of Mars acquired by the Viking Orbiter missions. The images have resolutions ranging from 173 meters per pixel to 32 meters per pixel. To make the most accurate measurements we elected to focus our study on two frames, 586B34 and 586B36 (34 and 36, Figures 1a and 1b), comprising an area where a greater concentration of the individual domes is more visible above the surrounding sediments.

METHODS

Frames 34 and 36 were mapped in order to develop an understanding of the regional geomorphology and stratigraphy. Understanding the regional geology is important for constraining the types of factors that might affect interpretation of dome morphology. It is particularly important to determine whether or not the domes are partially buried by surrounding sediments.

In our study area, 649 domes, comprising numerous dome clusters, were identified as either elliptical or circular in shape. For those that appeared circular one diameter was measured. Those that appeared elliptical were

Mantle Downwelling. A plateau-shaped highland is produced in this model by crustal shortening over a region of mantle downwelling [*Bindschadler et al.*, 1992]. Here, ridges form sub-parallel to the highland boundary due to radial compression, which also causes an overall increase in elevation [*Bindschadler et al.*, 1992]. As this process eventually begins to slow and end, it is also predicted that extension and an overall decrease in elevation will occur as the highland begins to spread under its own weight [*Bindschadler et al.*, 1992]. *Parmentier and Hess* [1992] and *Head et al.* [1994] have proposed a depleted mantle layer overturn mechanism to begin such a downwelling event. The basic operating premise is that an accumulated depleted mantle layer from basaltic volcanism will eventually become negatively buoyant and founder, creating a mantle downwelling site [*Parmentier and Hess*, 1992; *Head et al.*, 1994]. There is good agreement between the structure predicted by this model and what we have observed in northern Ovda Regio. The prediction of sub-parallel ridges as the formative unit of the highland, and the subsequent sequence of structure, all agree with our observations, indicating that this region could have formed during such an event.

REFERENCES CITED

Bindschadler, D.L., G. Schubert, and W.M. Kaula, 1992, Coldspots and hotspots: Global tectonics and mantle dynamics of Venus: Journal of Geophysical Research, v. 97, p. 13,495-13,532.

Ford, J.P., J.J. Plaut, C.M. Weitz, T.G. Farr, D.A. Senske, E.R. Stofan, G. Michaels, and T.J. Parker, 1993, Guide to Magellan Image Interpretation: NASA, Jet Propulsion Laboratory.

Head, J.W. and L.S. Crumpler, 1987, Evidence for divergent plate-boundary characteristics and crustal spreading on Venus: Science, v. 238, p. 1,380-1,385.

Head, J.W. and M. Ivanov, 1993, Tessera terrain on Venus: Implications of tessera flooding models and boundary characertistics for global distribution and mode of formation: Lunar and Planetary Science Conference, v. 24, p. 619-620.

Head, J.W., E.M. Parmentier, and P.C. Hess, 1994, Venus: Vertical accretion of crust and depleted mantle and implications for geological history and processes: Planetary and Space Science, v. 42, p. 803-811.

Head, J.W., 1995, Tectonic facies in Venus tessera terrain: Classification and interpretation of sequence of deformation: Lunar and Planetary Science Conference, v. 26 ,p. 579- 580.

Ivanov, M.A. and J.W. Head, 1996, Tessera Terrain on Venus: A survey of the global distribution, characteristics, and relation to surrounding units from Magellan data: Journal of Geophysical Research, v. 101, p. 14, 861-14,908.

Kiefer, W.S. and B.H. Hager, 1991, A Mantle Plume Model for the Equatorial Highlands of Venus: Journal of Geophysical Research, v. 96, p. 20,947-20,966.

Parmentier, E.M., and P.C. Hess, 1992, Chemical differentiation of a convecting planetary interior: Consequences for a one plate planet such as Venus: Geophysical Research Letters, v. 19, p. 2015-2018.

Phillips, R.J., R.E. Grimm, and M.C. Malin, 1991, Hot-spot evolution and the global tectonics of Venus: Science, v. 252, p. 651-658.

Schaber, G.G., R.G. Strom, H.J. Moore, L.A., Soderblom, R.L. Kirk, D.J. Chadwick, D.D. Dawson, L.R. Gaddis, J.M. Boyce, and J. Russell, 1992, Geology and distribution of impact craters on Venus: What are they telling us?: Journal of Geophysical Research, v. 97, p. 13,257-13,301.

Sotin, C., D.A. Senske, J.W. Head, and E.M. Parmentier, 1989, Terrestrial spreading centers under Venus conditions: Evaluation of a crustal spreading model for western Aphrodite Terra: Earth and Planetary Science Letters, v. 95, p. 321-333.

Strom, R.G., G.G. Schaber, and D.D. Dawson, 1994, The global resurfacing of Venus: Journal of Geophysical Research, v. 99, p. 10,899-10,926.

Tormanen, T., 1993, Complex ridged terrain-related ridge belts on Venus: Global distribution and classification: Lunar and Planetary Science Conference, v. 24, p. 1439-1440.

measured along the length of both their long and short axes. The ratio between the short and long axis, also known as the aspect ratio or ellipticity ratio, of each elliptical dome was calculated. In addition, the orientation of each long axis was recorded. Other data collected include percentages of domes with central pits, spatial density of the domes to determine if there is regularity in their spatial distribution, and the orientations of linear troughs and fractures in the region. Adobe Photoshop 3.0 and NIH Image 1.6 were the computer software used to obtain data on the domes, dome clusters, and fractures.

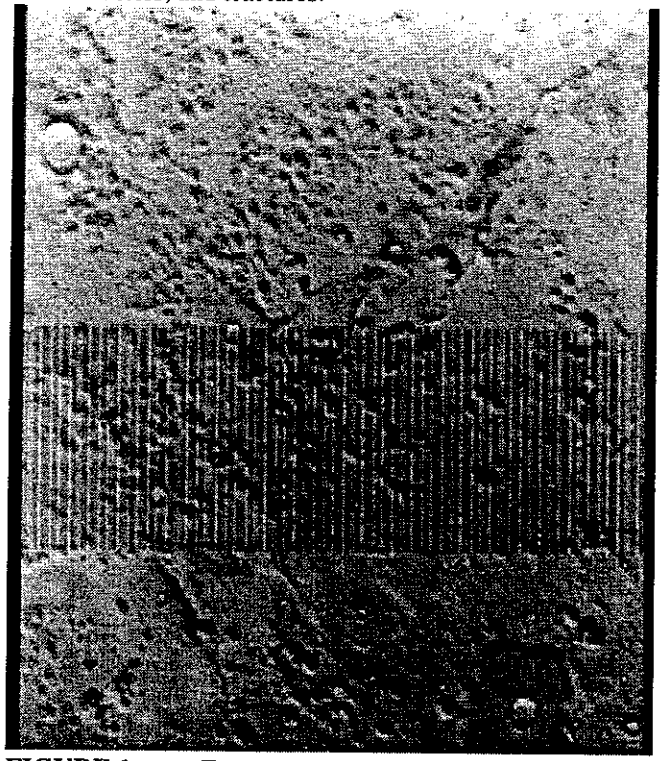

FIGURE 1a. Frame 34
Taken from the Viking II Orbiter data; resolution of the frame is 0.032 kilometers per pixel. The frame is approximately 37.2 kilometers by 33.8 kilometers.

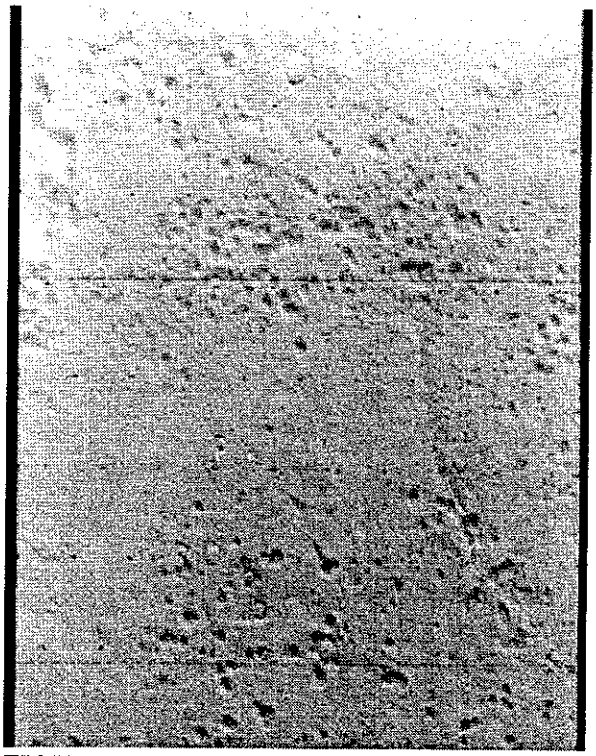

FIGURE 1b. Frame 36
Taken from the Viking II Orbiter data; resolution of the frame is 0.031 kilometers per pixel. The frame is approximately 36.0 kilometers by 32.7 kilometers.

RESULTS

In the Arrhenius Region, scattered steep scarps separate areas of higher elevation from areas of lower elevation. Compared to lower-elevation areas, the higher elevation areas are characterized by smaller domes, sediment-filled craters, rampart craters with smooth circumferences, and interdome and crater areas that are smooth-textured plains. The rampart craters are also identified as infilled craters with smooth flat crater floors, subdued caldera rims, and absence of an ejecta blanket. On the opposite side of the scarps, lower elevation areas are characterized by larger domes, pristine craters, and pedestal craters with irregular circumferences, associated with rough-textured plains that exhibit fractures and a trough. Pristine craters have prominent undulating ejecta blankets with sharply defined crater rims, which are consistent with geologically recent impact features. Here pedestal craters are also identified by a well-defined ejecta blanket that is more resistant than the more friable surrounding sediments. The pristine and pedestal craters appear similar because the pristine ones are freshly created and the pedestal craters are comparatively recently exhumed by aeolian deflation; however, they both appear in lower elevation topography. Rampart craters also present in the lower elevated areas appear as more clearly defined ejecta blankets with evidence of some flow structure. The ejecta features suggest that the surrounding sediment is composed of ice-rich material, whose melting caused the fluidized appearance of the ejecta. Based on this

observation, we conclude that exhumation has occurred in at least the lower elevation areas. Therefore, Arrhenius is more resonably interpreted as an area of deposition which is now undergoing partial exhumation through aeolian deflation (Tanaka and Leonard, 1995).

Table I, presents dome measurements and other data from the Arrhenius Region in comparison with several terrestrial volcanic cinder cone fields, including the Ethiopian Rift, Tepic Rift (Mexico), Transtensional Mexican Volcanic Belt (MVB), Canary Archipelago, and Mount Etna (Tibaldi, 1995).

TABLE 1: Dome Parameters and Comparison of the Arrhenius Region with Terrestrial Cinder Cone Fields

	Our Frames 34 & 36		Ethiopia Rift		Tepic Rift		Transtensional MVB		Canary Islands		Mount Etna	
	Min	Max	Min	Max	Min	Max	Min	Max	Min	Max	Min	Max
Number of domes	649		57		100		826		144		188	
Length of elliptical base:												
short diameter, km	0.22	1.09	0.10	1.50	0.19	1.70	0.16	1.25	0.05	0.10	0.04	0.70
long diameter, km	0.37	1.89	0.10	1.50	0.22	1.90	0.16	1.90	0.08	1.20	0.80	0.90
Total average basal diameter, km	0.61		0.65		0.80		0.59		0.36		0.29	
% of circular domes	60.4%		26.0%		28.0%		6.0%		8.0%		36.0%	
% of elliptical domes	39.6%		74.0%		72.0%		94.0%		92.0%		64.0%	
Aspect (ellipticity) ratio	0.35	0.99	0.50	1.00	0.34	1.00	0.41	1.00	0.33	1.00	0.33	1.00
Average aspect (ellipticity) ratio	0.63		0.77		0.66		0.75		0.83		0.83	

DISCUSSION

When compared with data from Earth, it is clear that the dome morphologies in the Arrhenius region are consistent with a volcanic origin. This interpretation is based on analysis of orientations, diameter relationships, density, presence of a trough and fractures, central pits and dome aspect ratios. Because the average orientations of dome chains and elongate domes are nearly identical, in a northwest southeast orientation, it would appear that there is some regional process controlling their formation. We interpret the linear trough in frame 36 to be bounded by fractures that probably form a trough (located in Figure 1b, far right-hand margin one third of the way down). The fractures and trough, which is possibly a graben, both formed in one regional stress regime. The observed alignment and elongation of domes may be controlled by subsurface fissures that channeled magma up to the surface. These fissures exhibit the same alignment as the domes. There are also multiple aligned domes throughout the study area, all in approximately the same orientation as the individual domes and regional fractures. Considered collectively, these lines of evidence are strongly consistent with the argument that the domes are volcanic and that they may have erupted from a regional system of fissures.

Using the mapping results and morphologic data presented, two alternative volcanic hypotheses are suggested: cinder cones (Hodges, 1979; Plescia, 1980; Wood, 1979) and table mountains (Hodges, 1979), which are formed in different terrestrial environments (Figures 2a and 2b). A cinder cone origin implies that the domes were formed when magma erupted onto the surface. The regional stratigraphy would require that dome emplacement preceded sediment deposition and subsequent erosion (Figure 2a). A table mountain origin implies eruption beneath an ice-rich layer. There is direct evidence for a permafrost layer within the sediments (i.e. the rampart craters and their fluidized ejecta blankets), which is consistent with a table mountain origin. The sequence of events would be deposition of sediment sheet and permafrost, eruption of magma to form the domes beneath the surface, then exhumation of the sediment sheet to reveal the domes (Figure 2b). Because of the resolution of our images, we are unable to determine which of these volcanic processes is most likely to have created the Arrhenius domes. From the

evidence we have found, we believe that this area is a result of volcanism, but the exact type is not clear. Further work to constrain the relative timing of the sediment sheet and domes will help discriminate between the two possibilities.

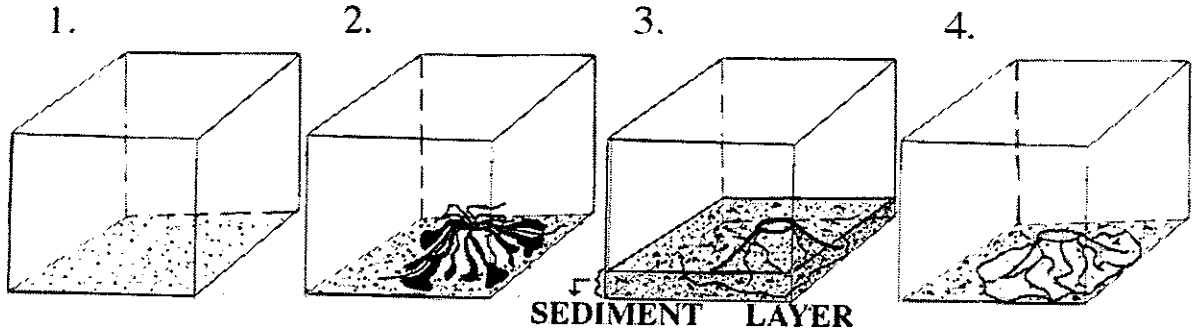

Figure 2a. Interpreted sequence of events for Cinder Cone origin:
(1) Original surface; (2) Cone formation and eruption on surface; (3) Sediment sheet burying cone; (4) Partial exhumation of cone.

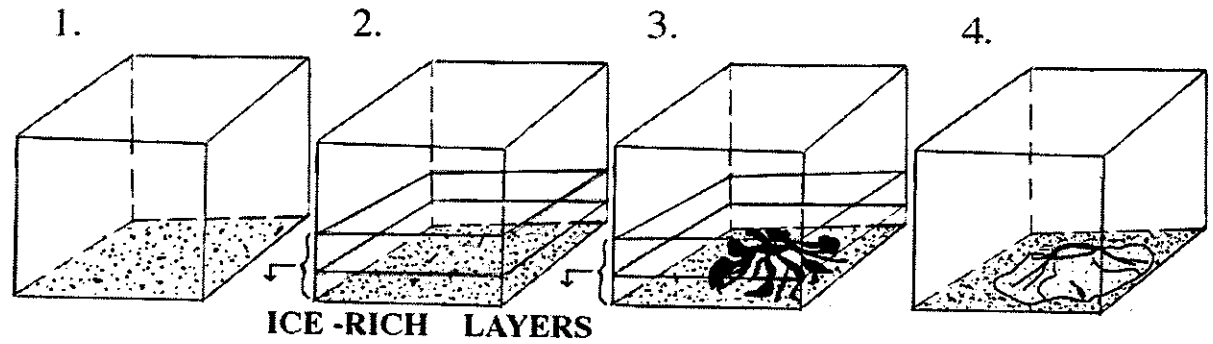

Figure 2b. Interpreted sequence of events for Table Mountain origin:
(1) Original surface; (2) Emplacement of ice-rich sediments; (3) Sub-surface eruption; (4) Partial exhumation of cone.

REFERENCES CITED

Allen, C. C., 1979, Volcano/ice interactions Mars: *Journal of Geophysical Research, v. 84*, p. 8048-8059.

Frey, H., and Jarosewich, M., 1981, Martian pseudocraters: Searching the northern plains, *Lunar and Planetary Science Conference, v. 12*, p. 297-299.

Frey, H., Lowry, B., and Chase, S., 1979, Pseudocraters on Mars: *Journal of Geophysical Research, v. 84*, p. 8075-8086.

Hodges, C.A., 1979, Some lesser volcanic provinces on Mars: *NASA Tech*nical *Memorandum, v. 80339*, p. 247-249.

Hodges, C.A., and Moore, H.J., 1994, Atlas of Volcanic Landforms on Mars: United States Government Printing Office, Washington, p. 168-172.

Judson, S., and Rossenbacher, L., 1979, Geomorphic role of ground ice on Mars: *NASA Tech*nical *Memorandum, v. 80339*, p. 229-231.

Plescia, J.B., 1980, Cinder cones of Isidis and Elysium: *NASA Tech*nical *Memorandum, v. 82385*, p. 263-265.

Tibaldi, A., 1995, Morphology of pyroclastic cones and tectonics: *Journal of Geophysical Research, v. 100*, p. 24521-24535.

Tanaka, K. L., and Leonard, G.J., 1995, Geology and Landscape evolution of the Hellas region of Mars: *Journal of Geophysical Research, v. 100*, p. 5407-5432.

Wood, C.A., 1979, Monogenetic volcanoes of the terrestrial planets: *Proceedings of the Lunar and Planetary Science Conference, v. 10*, p. 2815-2840.

Viscosity of venusian lava flows: constraints from fractal dimension and chemical composition

Holli Frey
Department of Geoscience, Franklin & Marshall College, Lancaster, PA 17604
Faculty sponsor: Donald U. Wise, Franklin & Marshall College

Alexandra E. Krull
Department of Geology, Pomona College, Pomona ,CA 91711
Faculty sponsor: Eric Grosfils, Pomona College

William A. Pike
Department of Geology, Carleton College, Northfield, MN 55057
Faculty sponsor: Mary Savina, Carleton College

INTRODUCTION

Fractal analysis can be used to quantify the morphology of lava flow margins. Work by *Bruno* et al. [1992] and *Bruno and Taylor* [1995] has demonstrated that terrestrial and venusian flows of basaltic composition are fractal and that fractal dimension can be used to categorize flows as a'a, pahoehoe, or transitional. One determinant of flow type and rheology, which are reflected in flow margin, is lava viscosity [*Bruno* et al. 1994]. Viscosity is dependent upon chemical composition, which at several sites on Venus has been measured by Venera and Vega landers. This study attempts to associate the fractal geometry of venusian lava flows with chemical data derived from lander measurements and terrestrial analogs. We hypothesize that a low-viscosity lava will produce a more sinuous flow margin, thus having a greater fractal dimension than a viscous lava. We endeavor to develop fractal analysis as a tool for use in the determination of lava viscosity and composition where lander data are unavailable.

METHODS

Radar images taken by the Magellan orbiter are used to find and analyze the lava flows. Because flows are self-similar over several orders of magnitude [*Bruno and Taylor*, 1995], we are able to use both F-MIDRS (Full-Resolution Mosaicked Image Data Records) with a resolution of 75 meters per pixel, and C1-MIDRS (Compressed-Once Mosaicked Image Data Records) with a resolution of 225 meters per pixel in our analysis. Our sample contains 72 flow margins, all of which have slopes of less than one degree and are free of cratering and tectonic or volcanic deformation. Thirteen of the flow margins are located within the 300 km landing ellipses of the Vega 2, Venera 8, Venera 13, and Venera 14 landers. We prepared three independent traces of each flow margin in the sample.

Each flow margin trace was imported into Fractal Dimension Calculator version 1.0 [*Bourke*, 1993] for analysis. This software program uses a box-counting algorithm to analyze fractal nature of flow margins. This method overlays a series of grids composed of squares with uniform side length s over the flow front trace. The relationship $L=N(s)*s$ approximates the length L of the flow margin trace, where $N(s)$ is the number of boxes of side length s needed to cover the trace. As s decreases, $N(s)$ increases according to a power law and L becomes an increasingly more accurate approximation of the length of the curve [*Pruess*, 1995]. The power that reflects the nonlinear growth in $N(s)$ is the fractal dimension D of the curve. As D increases, the sinuosity or the amount of a plane filled by the flow margin increases. Venusian lava flows have been shown to have D between 1.04 and 1.24 [*Bruno and Taylor*, 1995].

We specified ten box sizes covering three orders of magnitude. The slope of a modified Richardson plot, showing log $[N(s)]$ versus log $[1/s]$ is our approximation of D. The mean D of three traces of each flow margin is adopted as each flow's fractal dimension.

To estimate the original viscosity of the landing site rock we used the procedure outlined in detail in *Shaw* [1972]. This viscosity estimation technique employs rock chemistry, water weight percent, the temperature of the original melt, and assumes no exsolution of volatiles. Rock chemistry is given by the weight percent major element